N86-30175

ANALYTICAL PREDICTION OF LABYRINTH-SEAL-FLOW-INDUCED ROTOR EXCITATION FORCES

C. Rajakumar and E. Sisto
Stevens Institute of Technology
Hoboken, New Jersey 07030

An analytical method to calculate the rotor excitation forces arising from labyrinth seals is presented. The objective is to model the gas flow through the seal clearance passages and cavities when the rotor is positioned eccentric relative to the stator center. The seal flow model used in the analysis yields solutions which validate the experimentally observed influence of seal parameters on seal forces reported in the literature. The analytically predicted seal pressure distributions and forces have been compared with published experimental results.

INTRODUCTION

While performing the function of sealing, labyrinth seals have been identified as a potential source of destabilizing forces which cause self excited rotor whirl of turborotors. Typically these seals are employed to effect sealing of the working fluid between two stages of a compressor or turbine and in adjacent cooling air compartments which are maintained at different pressures. Labyrinth seals which have a configuration as shown in figure 1 are designed to minimize the leakage flow by successively expanding the gas past the orifice-like clearance passages at the seal fin locations.

An analytical model describing the excitation of turborotors by labyrinth seals was first published by Alford (ref. 1). In the recent literature (ref. 2 to 7) experimental and analytical methods of predicting labyrinth seal forces have been reported. Experimental results presented by Benckert and Wachter (ref. 2) show that a restoring force along the line of centers and a lateral force normal to the line act on the rotor when the rotor center is displaced to an eccentric position with respect to the seal center as shown in figure 2. The present work is aimed at analytically predicting these seal forces which result from the circumferentially varying pressure distributions within the seal cavities.

SYMBOLS

C	seal radial clearance
Cc	orifice flow coefficent
Ce	energy recovery factor
Co	nominal radial clearance
e	rotor eccentricity
e_r	eccentricity ratio (e/Co)
f	circumferential flow area
Fr, Ft	radial and tangential seal forces
h	seal fin height

l	cavity width
m	number of circumferential nodes
N	rotor rpm
n	number of seal fins
P	pressure (Po- seal inlet, Pe- seal exit)
q	axial mass flow rate per unit circumferential length
R	gas constant
Re	reynolds number
Rs	rotor radius
t	axial pitch
T	gas temperature
u	circumferential flow velocity
u_o	inlet swirl velocity
U	length of wetted surface
α	flow coefficient
λ	friction coefficient at the walls
μ	coefficient of viscosity
ϕ	reference angle shown in figure 2
ρ	gas density
τ	shear stress
θ	circumferential coordinate
ω	angular velocity of rotor rotation
Subscripts	
i	fin and cavity number designations
j	circumferential node number
r	rotor
s	stator

GOVERNING EQUATIONS

The intricate flow path of labyrinth seals, combined with the asymmetry caused by rotor eccentricity complicate the analysis employing fundamental fluid mechanics governing equations. A relatively simpler set of labyrinth seal governing equations derived by Kostyuk (ref. 8) are employed in the analysis here. For the fluid macro-element shown in figure 1, the following conservation of mass and circumferential momentum equations are derived, neglecting the curvature effect for small clearance-to-radius ratios.

$$\frac{\partial}{\partial t}(\rho_i f_i) + \frac{1}{Rs}\frac{\partial}{\partial \theta}(\rho_i u_i f_i) + (q_{i+1} - q_i) = 0 \qquad (1)$$

$$\frac{\partial}{\partial t}(\rho_i u_i f_i) + \frac{1}{Rs}\frac{\partial}{\partial \theta}(\rho_i u^2_i f_i) + (q_{i+1}\, u_i - q_i u_{i-1})$$

$$= -\frac{f_i}{Rs}\frac{\partial P_i}{\partial \theta} + (\tau_{ri} U_{ri} - \tau_{si} U_{si}) \qquad (2)$$

Frictional resistance at the seal walls are calculated using the following relationships.

$$\tau_{si} = \lambda_{si} \frac{\rho_i u_i^2}{2}, \quad \tau_{ri} = \lambda_{ri} \frac{\rho_i (\omega Rs - u_i)^2}{2} \tag{3}$$

where:

$$\lambda = \frac{8}{Re} \quad 0<Re\leq 1000, \qquad \lambda = \frac{0.045}{Re^{.25}} \quad 1000 < Re$$

The Reynolds numbers are given by:

$$Re_{si} = \frac{|u_i| h_i \rho_i}{2\mu}, \quad Re_{ri} = \frac{|\omega Rs - u_i| h_i \rho_i}{2\mu} \tag{4}$$

Proper signs are attached to the friction coefficient λ based on the relative velocity of the fluid with respect to the rotor and stator walls. Assuming isothermal flow process, Martin's (ref. 9) leakage flow equation for small pressure drop accross each fin is given by:

$$q_i = \alpha_i (P^2_{i-1} - P^2_i)^{.5} \tag{5}$$

where:

$$\alpha_i = \frac{1}{\sqrt{RT}} \frac{Cc_i}{(1-Ce_i)^{.5}} \tag{6}$$

Orifice flow coefficients Cc for annular orifices presented by Vermes (ref. 10) have been used in the calculations. The residual energy factor Ce accounts for the part of the kinetic energy in the leakage flow from the (i-1)th orifice that is present at the inlet to the i-th orifice. Representing the orifice flow by one half of a flat symmetrical jet, Vermes (ref. 10) derived the following expression for the residual energy factor:

$$Ce_i = \frac{8.52}{(l_i/C_i) + 7.23} \tag{7}$$

Equations (1), (2), (5) and the ideal gas relationship

$$P_i = \rho_i RT \tag{8}$$

form the system of equations to be solved for the circumferential pressure distribution resulting due to the rotor eccentricity. Although figure 1 shows fins on the rotor, the equations derived are also valid for a labyrinth with fins on the stator.

NUMERICAL PROCEDURE

For the rotor undergoing steady rotational motion about a given eccentric position (fig. 2), we can drop off the time derivative terms in equations (1) and (2). After substituting for q_i and ρ_i from equations (5) and (8), equations (1) and (2) become:

$$\frac{1}{RTRs}\frac{d}{d\theta}(P_i u_i f_i) + \alpha_{i+1}C_{i+1}(P^2_i - P^2_{i+1})\cdot 5$$

$$- \alpha_i C_i \quad (P^2_{i-1} - P^2_i)\cdot 5 = 0 \tag{9}$$

$$\frac{1}{RTRs}\frac{d}{d\theta}(P_i u^2_i f_i) + \alpha_{i+1} C_{i+1}(P^2_i - P^2_{i+1})\cdot 5\, u_i$$

$$- \alpha_i C_i (P^2_{i-1} - P^2_i)\cdot 5 u_{i-1} + \frac{f_i}{R_s}\frac{dP_i}{d\theta} + (\tau_{si}U_{si} - \tau_{ri}U_{ri}) = 0 \tag{10}$$

The seal clearance and circumferential flow area for the eccentric rotor configuration are given by:

$$C_i = Co_i - e\cos\theta \tag{11}$$

$$f_i = l_i\,(h_i + Co_i - e\cos\theta) \tag{12}$$

Equations (9) and (10) are nonlinear ordinary differential equations to be solved to get the pressure and velocity distributions, $p_i\ (\theta)$ and $u_i\ (\theta)$ in each seal cavity.

After introducing the central finite difference approximations given below we divide the circumferential coordinate length, $Rs\theta$ into m equal parts.

$$\frac{dP_i}{d\theta} = \frac{P_{ij+1} - P_{ij-1}}{2\Delta\theta} \tag{13}$$

$$\frac{du_i}{d\theta} = \frac{u_{ij+1} - u_{ij-1}}{2\Delta\theta} \tag{14}$$

The resulting system of nonlinear algebraic equations are represented symbolically as:

$$F\ (P_{ij},\ u_{ij}) = 0 \tag{15}$$

$$G\ (P_{ij},\ u_{ij}) = 0 \quad i=1,2..(n-1) \quad j=1,2..m \tag{16}$$

Equations (15) and (16) are solved employing the Newton Raphson iteration procedure in the multidimensional space formed by the variables P_{ij} and u_{ij}. After dropping the second and higher order terms from the Taylor series expansions of equations (15) and (16), we arrive at the iteration scheme given by:

$$\begin{Bmatrix} P_{ij} \\ u_{ij} \end{Bmatrix}_{k+1} = \begin{Bmatrix} P_{ij} \\ u_{ij} \end{Bmatrix}_k - \begin{bmatrix} \frac{\partial F}{\partial P_{ij}} & \frac{\partial F}{\partial u_{ij}} \\ \frac{\partial G}{\partial P_{ij}} & \frac{\partial G}{\partial u_{ij}} \end{bmatrix}^{-1}_k \begin{Bmatrix} F(P_{ij},\ u_{ij}) \\ G(P_{ij},\ u_{ij}) \end{Bmatrix}_k \tag{17}$$

By assuming an initial guess for the vector $[P_{ij}\ u_{ij}]_k$, the Jacobian matrix and the function values are evaluated to calculate the new vector of variables $[P_{ij}\ u_{ij}]_{k+1}$. The iterations are continued until the change in each component of the solution vector is less than a predetermined error value. The seal forces are obtained by integration of the pressure distribution over the rotor surface using the summation equations given by:

$$Fr = Rs\Delta\theta \sum_{i=1}^{n-1} l_i \sum_{j=1}^{m} P_{ij} \cos\theta_j \tag{18}$$

$$Ft = Rs\Delta\theta \sum_{i=1}^{n-1} l_i \sum_{j=1}^{m} P_{ij} \sin\theta_j \tag{19}$$

RESULTS

Seal cavity pressure distributions obtained were compared with the experimental results of Leong and Brown (ref. 4) shown in figure 3. The 11-cavity seal having fins on the stator with inlet and exit pressure of Po=2.914 bar, Pe=1 bar was investigated at a rotor speed of 7504 rpm and eccentricity ratio of 0.6. The analytically predicted pressure distribution patterns in the first two seal cavities are in agreement with the experimentally measured patterns, with a peak pressure occuring near the 180 degrees location in the first cavity while the pressure is minimum near this location in the second cavity. Pressure levels predicted by the theory beyond the first three cavities are in fair agreement with the experimental results. The difference in cavity pressure levels between the theory and experiment is attributable to possible difference between the orifice flow coefficients used in the calculations and the actual flow coefficients in the experiment. Also, possible random variations of the seal clearance at successive fin locations in the test seal could contribute to the difference between the experimental and analytical results.

The experimental results of Benckert and Wachter (ref. 2) were used to verify the seal forces calculated analytically. Figures 5 and 6 show the variation of seal forces with eccentricity ratio for a 17-cavity seal with fins on the stator. Tangential forces generated when the rotor rotates at 9482 rpm and 4773 rpm, for the seal inlet and exit pressures of Po=1 bar, Pe=1 bar are shown in figure 4(a). The negative eccentricity ratios indicate that the rotor center has been displaced along the negative x-axis in figure 2. The analytically predicted tangential seal forces are in good agreement with the experimental results showing an average deviation of about 16 percent, excluding the zero eccentricity ratio case where the experimental results show a nonzero force. Radial forces predicted by the analysis are shown in figure 4(b); experimental results on radial forces were not reported in the reference for the case investigated. These results show that the seal force magnitudes increase with rotor rotational speed for any given eccentricity ratio. The tangential forces act in a direction that would initiate or promote forward whirl motion of the rotor center. The radial forces are decentering where they tend to push the rotor away from the seal center.

The seal forces variation with eccentricity ratio for zero rotor speed, but nonzero swirl velocity at the seal inlet are presented in figures 5(a) and 5(b). The seal pressures in this case are Po=2.041 bar, Pe=1 bar. The tangential seal forces have been predicted quite close to the experimental results, the maximum difference being 17 percent. The radial forces from the experiment, again were not

reported in the reference. The two different inlet swirl velocities investigated show that the seal forces increase with the inlet swirl velocity and appreciable magnitudes of tangential forces are generated which would promote forward whirl instability in rotor systems. The radial forces in this case are of relatively small magnitude and they act in a centering direction tending to restore the rotor center back to the seal center.

CONCLUSIONS

Employing the seal flow governing equations derived by Kostyuk (ref. 8), methods of predicting seal forces for an infinitesimal eccentricity have been reported in the literature where seal stiffness coefficients are presented. In this analysis the radial and tangential components of seal forces for large eccentricity ratios have been predicted, for the first time, employing Kostyuk's equations. The analysis yields results which validate the experimentally observed variation of seal forces with rotor eccentricity, inlet swirl velocity and rotor rotational speed. The tangential force components predicted by the theory, especially the swirl flow-induced forces are in good quantitative agreement with the experimental results. The analysis also shows the nonlinear dependence of the forces with eccentricity beyond $e_r \simeq .4$. This behavior needs to be given appropriate consideration in large amplitude rotor dynamic investigations where nonlinear stability problems may be encountered.

REFERENCES

1. Alford, J.S.: Protecting Turbomachinery From Self Excited Rotor Whirl. ASME Journal of Engineering for Power, Vol. 87, No. 4, Oct. 1965, pp. 333-344.

2. Benckert, H.; and Wachter, J.: Flow Induced Spring Coefficients of Labyrinth Seals for Application in Rotor Dynamics. NASA CP 2133, 1980, pp. 189-212.

3. Hauck, L: Exciting Forces Due to Swirl Type Flow in Labyrinth Seals. Proceedings of the IFTOMM Conference on Rotordynamics, Rome, Sept. 1982.

4. Leong, Y.M.M.S.; and Brown, R.D.: Circumferential Pressure Distributions in a Model Labyrinth Seal. NASA CP 2250, 1982, pp. 223-241.

5. Leong, Y.M.M.S.; and Brown, R.D.: Experimental Investigations of Lateral Forces Induced by Flow Through Model Labyrinth Glands. NASA CP 2338, 1984, pp. 187-210.

6. Murphy, B.T.; and Vance, J.M.: Labyrinth Seal Effects on Rotor Whirl Instability. Institution of Mechanical Engineers CP C306/80, 1980, pp. 369-373.

7. Wright, D.V.: Labyrinth Seal Forces on a Whirling Rotor. ASME Publication on Rotor Dynamical Instability AMD, Vol. 55, 1983, pp. 19-31.

8. Kostyuk, A.G.: A Theoretical Analysis of the Aerodynamic Forces in the Labyrinth Glands of Turbomachines. Teploenergetica, 19(11) 29-33, 1972, pp. 39-44.

9. Martin, H.M.: Labyrinth Packings. Engineering, Vol. 85, Jan. 10, 1908, pp. 35-38.

10. Vermes, G: A Fluid Mechanics Approach to the Labyrinth Seal Leakage Problem. ASME Journal of Engineering for Power, Vol. 83, April 1961, pp. 161-169.

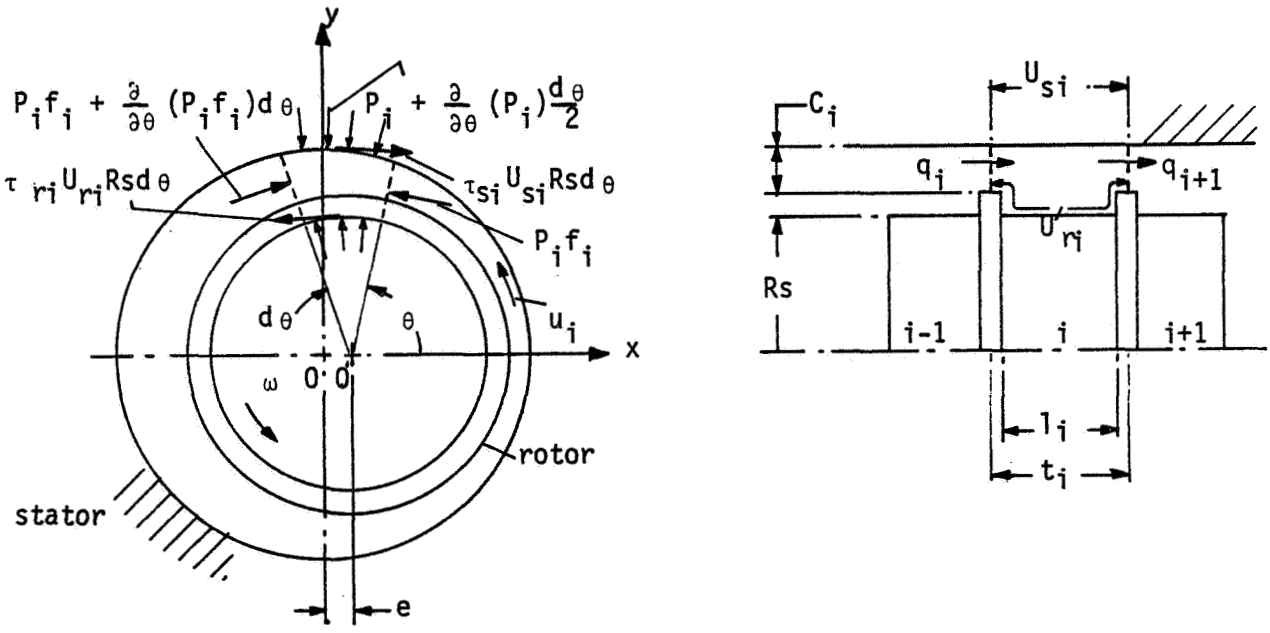

Figure 1. - Labyrinth seal fluid element.

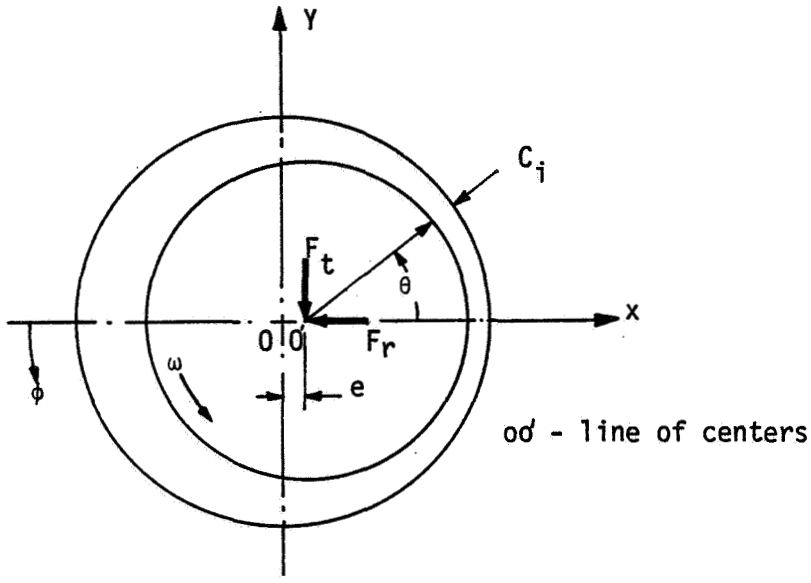

Figure 2. - Seal forces.

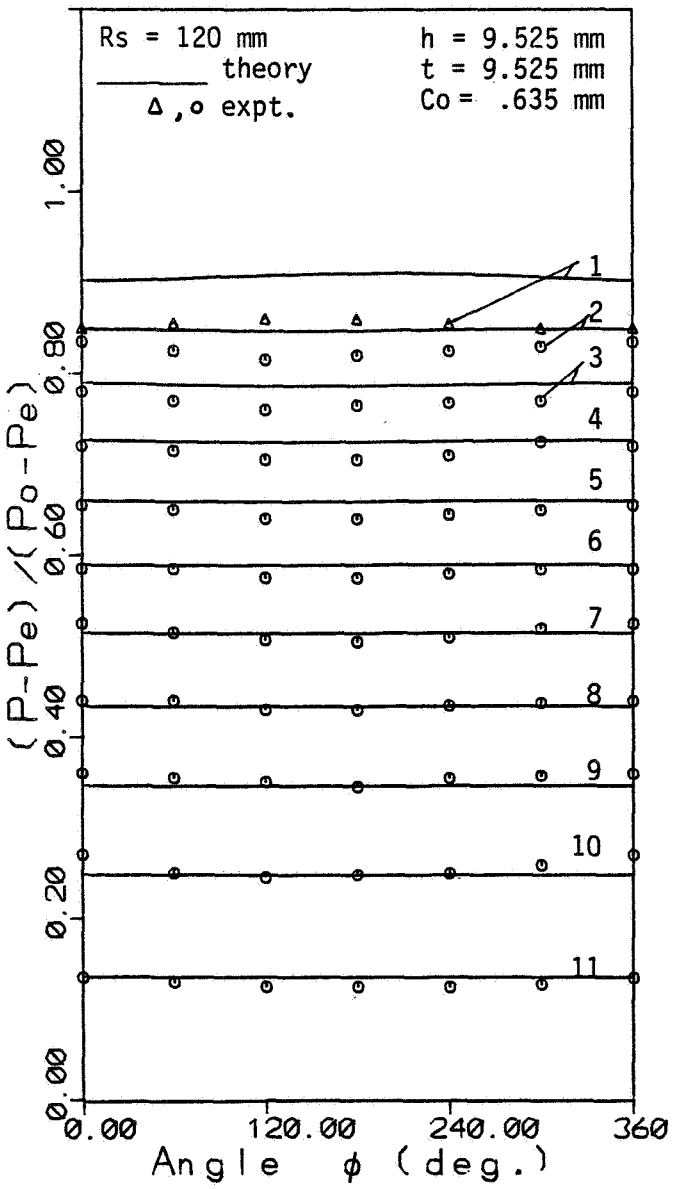

Figure 3. - Seal pressure distribution.

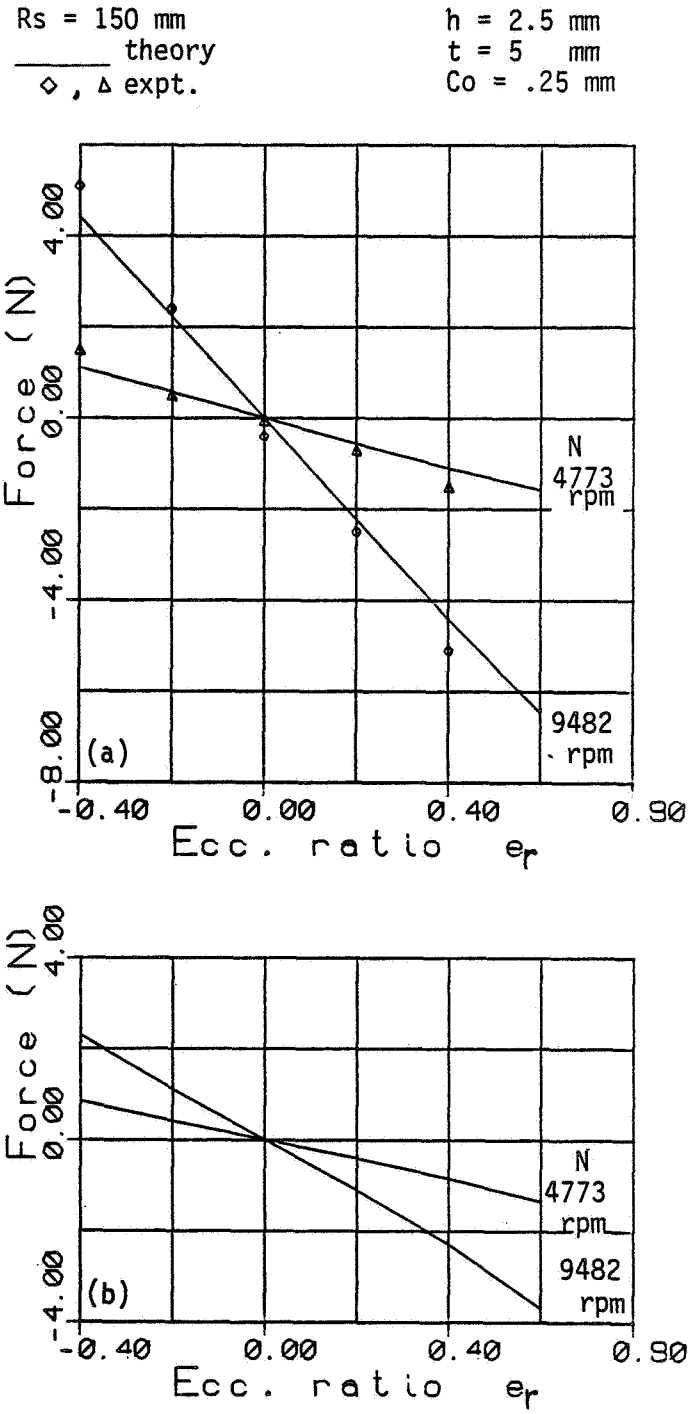

(a) Tangential force Ft.
(b) Radial force Fr.

Figure 4. - Seal forces with variable rotor speed.

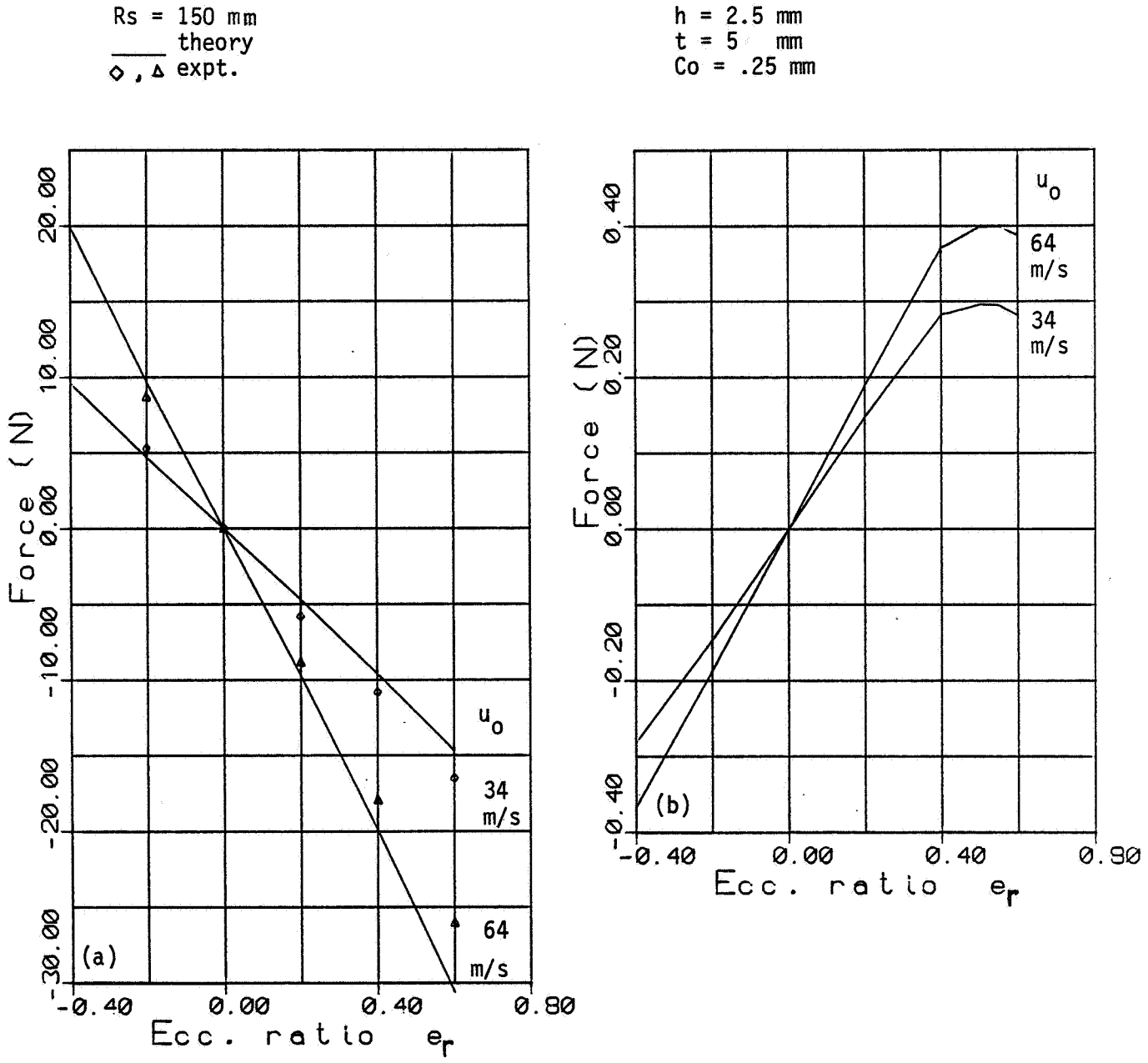

(a) Tangential force Ft.
(b) Radial force Fr.

Figure 5. - Seal forces with variable inlet swirl velocity.